[1,2,*]**Brahim Gharbi,**

[3,4]**Adel Taabouche,**

[2,5]**Maroua Brella,**

[1,6]**Fatiha** Chelgham,

[1,2]**Abdellatif Mamanou**

Synthesis and Characterization of ZnO-CuO Nanocomposites Thin Film for Optoelectronics Applications
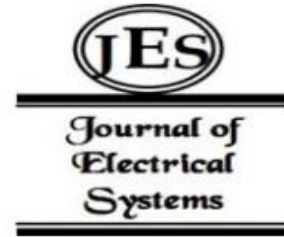
Abstract: In this work, the spray pyrolysis technique on glass substrates at 480°C was effectively used to generate ZnO, CuO, and n-ZnO/p-CuO nanocomposite thin films. The structure of the ZnO thin films exhibited a hexagonal wurtzite type. In the visible region of the spectrum (400–700 nm), the resulting films had optical transmission ranging from 73% to 83% and optical band gap fluctuations of 3.23 to 3.25 eV. Analysis of the m-lines spectroscopy revealed that the obtained thin layers (ZnO, ZC3, and ZC7) exhibited two modes for both TE and TM polarizations across different molar percentages. This observation confirms the efficacy of the spray pyrolysis deposition technique in producing high-quality waveguides based on ZnO.

1. INTRODUCTION

Over the past few decades, the manufacture of materials based on transparent conductive oxides (TCO) nano-composites has aroused growing interest for their potential wide applications, such as super-capacitors [1], lithium-ion batteries [2, 3], high-sensitivity sensors [4, 5], UV photo-detectors [6], bio-components and others. Many studies have been conducted on pure transparent conductive oxide thin films, leading to a large body of work aimed at modifying and improving these films' characteristics through various techniques. Consequently, the synthesis of CuO–ZnO nanocomposites is highly advantageous for enhancing and adjusting the characteristics of pure CuO and ZnO metal oxide thin films. The zinc oxide (ZnO), is an n-type semiconductor material with a large direct band gap of 3.37 eV, a high refractive index, a high exciting binding energy of 60 meV, cheap cost, great photosensitivity, piezoelectricity, and high catalytic activity [7-9]. With a broad straight band gap of 1.2 eV, cupric oxide (CuO), a p-type semiconductor, is employed in thin films to create photovoltaic (PV) cells [10]. There are two tetragonal and monoclinic phases in CuO. CuO spontaneously stabilizes as a monoclinic phase in the majority of situations [11, 12].

2. EXPERIMENTAL

The required amounts of CuO and ZnO solutions were developed independently. As first precursors, copper acetate and zinc acetate dehydrate were used.

[1] Faculty of Hydrocarbons and Renewable Energies and Earth and Universe Sciences, The Kasdi Merbah University, Ouargla, 30000 Algeria.

[2]Laboratory of Radiation and Plasmas and Physical Surface (LRPPS), The Kasdi Merbah University, Ouargla, 30000 Algeria.

[3] Thin Films and Interfaces Laboratory, University of Fréres Mentouri Constantine, Constantine, 25000 Algeria.

[4] Département de Physique et Chimie, Ecole Normale Supérieure El Katiba Assia Djebar Constantine, Constantine, Algeria.

[5]Faculty of New Technologies and Information and Communication, Kasdi Merbah University, Ouargla, 30000, Algeria.

[6] Laboratory for the Valorization and Promotion of Saharan Resources, Kasdi Merbah University, 30000 Ouargla, Algeria.

[*]Email: gharbi.brahim@gmail.com

First, methanol alcohol was used to dissolve 0.1 M of zinc acetate dehydrate. Following 60 minutes of stirring at 800 C, CuO solution was added to ZnO at various molar ratios (mol%) of ZnO (ZnO (denoted ZC0), ZnO97:CuO3 (denoted as ZC3), and ZnO93:CuO7 (denoted as ZC7). ZnO (ZC0), ZC3, and ZC7 pure Thin films were deposited using the chemical spray pyrolysis technique. The substrate temperature was kept above the heater at 480 ºC.

3. RESULTS AND DISCUSSION

3.1. Diffraction Analysis of X-Rays

   X-ray diffraction was used to ascertain the nanomaterials' crystal structure. Figure 1 shows the XRD patterns of ZnO and CuO/ZnO nanocomposites at various copper concentrations. On the undoped ZnO (JCPDS N° 01-0750576) card, major peaks were seen at about 31.94°(100), 34.58°(002), 36.40°(101), 31.94°(100), 34.61°(002), 36.42°(101), 31.98°(100), 34.64°(002), and 36.45°(101) [13–15]. With the addition of Cu in ZnO, Note that the intensity of peaks (002) and (103) decreases. We also note that the intensity of the peaks (100), (101), (102) and (110) increases with the increase in Cu doping. For films ZC0, ZC3 and ZC7 the peak (002) is positioned on the diffractograms at 34.61, 34.55 and 34.89° respectively. The angular shift towards small values of θ is a consequence of the increase in the crystalline parameter c of the lattice. So because of the doping, the presence of stresses in the deposited films.
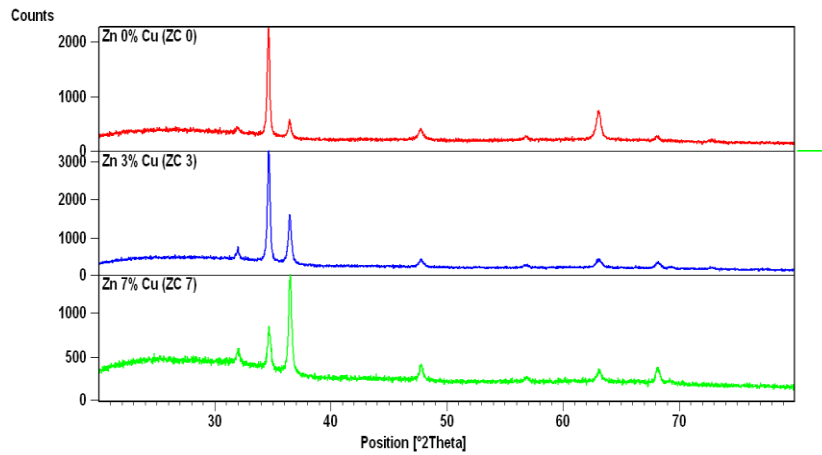
Fig. 1. XRD analysis of ZC7, ZC3, and ZC0 thin films of ZnO–CuO nanocomposite.

The XRD peaks unmistakably show that high-purity hexagonal wurtzite has formed (ZC0, ZC3 and ZC7) shows an example of the ZC0, ZC3, and ZC7 diffractogram's identification phases without the presence of metal oxide hydrates. Table 1.

Table 1. ZC7, ZC3, and ZC0 nanocomposite thin film values for Bragg angle 2θ, crystalline size D, and crystal orientations.

Cu (wt.%)	Phase	(%)	Ref. JCPDS	FWHM	Hkl	$2\theta_{int.}$	d_{hkl}	D_{XRD} (nm)
0	ZnO	100	01-075-0576	0.5377	100	31.9455	2.79955	16.2
				0.2256	002	34.5879	2.59121	41.8
				0.2955	101	36.4063	2.46585	30.7
3	ZnO	100	01-070-2551	0.3898	100	31.9445	2.79934	22.8
				0.2353	002	34.6191	2.58946	40.0
				0.3012	101	36.4265	2.46453	30.5
7	ZnO	100	01-089-0510	05133	100	31.9860	2.79580	17.0
				0.3535	002	34.6474	2.58690	25.4
				0.2947	101	36.4501	2.46298	31.2

   The absence of any diffraction peaks pertaining to impurities or secondary phases suggests that the precursor underwent full transformation into ZnO/CuO mixed metal oxides.

The Scherrer equation can be utilized to determine the strain and size of a crystal by calculating the mean crystallite size, which can be obtained from the full width at half maximum (FWHM) of a diffraction peak [16]:

$$DXRD = (K\lambda/\beta cos\theta) \tag{1}$$

where D is the crystal length, the diffraction angle of the (hkl) reflection is θ, the wavelength of the X-ray used is λ, K is the Scherrer constant, and β indicates the FWHM of the (hkl) reflection (in radians). Given that the Scherrer constant is influenced by the particle's shape.

The following formula may be used to determine β, which is obtained from the observed FWHM by convoluting a Gaussian profile that represents the specimen broadening βr [17] :

$$\beta_0^2 = \beta_i^2 + \beta_r^2 \tag{2}$$

where $\beta 0$ is the observed peak broadening in radians; βi the broadening due to instrumental factors, in radians and βr is the broadening due to crystallite size and lattice strain.

An estimate of the mean strain (ε) in a CuO/ZnO nanocomposite is given by the following equation [18]:

$$\varepsilon_{ZnO} = \left(\frac{c_{film} - c_0}{c_0}\right) \times 10^2 \tag{3}$$

where C_0 is the equivalent bulk value for ZnO (C_0 = 5.1948 Å) and c is the ZnO thin-film lattice constant as calculated using the standard spectrum (JCPDS File no. 01-075-0576).

$$\varepsilon_{CuO} = \left(\frac{a - a_0}{a_0}\right) \times 10^2 \tag{4}$$

where a_0 is the comparable bulk value for CuO and a is the lattice constant of CuO thin films.

Table 2 lists many crystalline properties.

Table 2. Mesh parameters and micro-stresses of ZC7, ZC3 and ZC0 films

Cu (wt.%)	Phase	Structure	a (Å)	a0 (Å)	c (Å)	c0 (Å)	V (Å³)
7	ZnO	Hexagonal	3.2513	3.2488	5.2035	5.2054	55.0059
3	ZnO	Hexagonal	3.2516	3.2490	5.2059	5.2070	55.0415
0	ZnO	Hexagonal	3.2521	3.2427	5.2081	5.1948	55.0817

ZC0 is thought to have an average crystallite size of 26,56 nm. While the anticipated thicknesses of ZC3 and ZC7 thin films are 31,1 and 24,53 nm, respectively.

3.2 UV-Visible Spectra Analysis

Figure 2 displays the UV-visible spectra of ZC0, ZC3, and ZC7 thin films that were produced at 480°C and put on glass substrates. The observations were made between 300 and 800 nm.
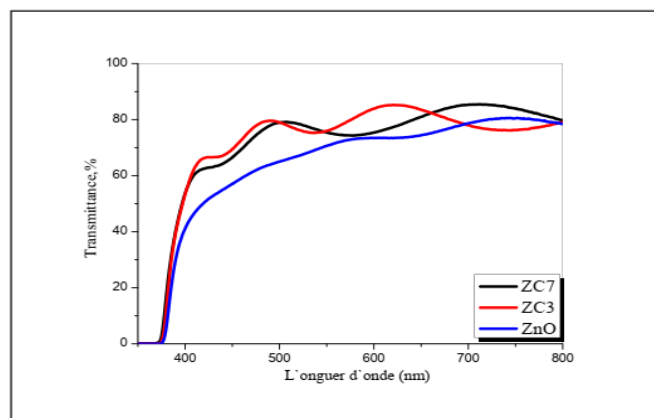
Fig. 2. The ZC0, ZC3, and ZC7 thin film transmittance spectra

The reading of the transmission spectra highlights two regions:

The films exhibit a high degree of transparency within the visible wavelength range of 400–700 nm, with an average optical transmittance ranging from 73 to 83%. ZC7 samples have an 83% transmittance, which is outstanding. Several writers have employed the approach of the first derivative of the transmittance (dT/dE) to determine the optical band gap Eg of the different samples [19–21]. Figure 3 displays the dT/dE vs. hv curves for the ZC0, ZC3, and ZC7 thin films.
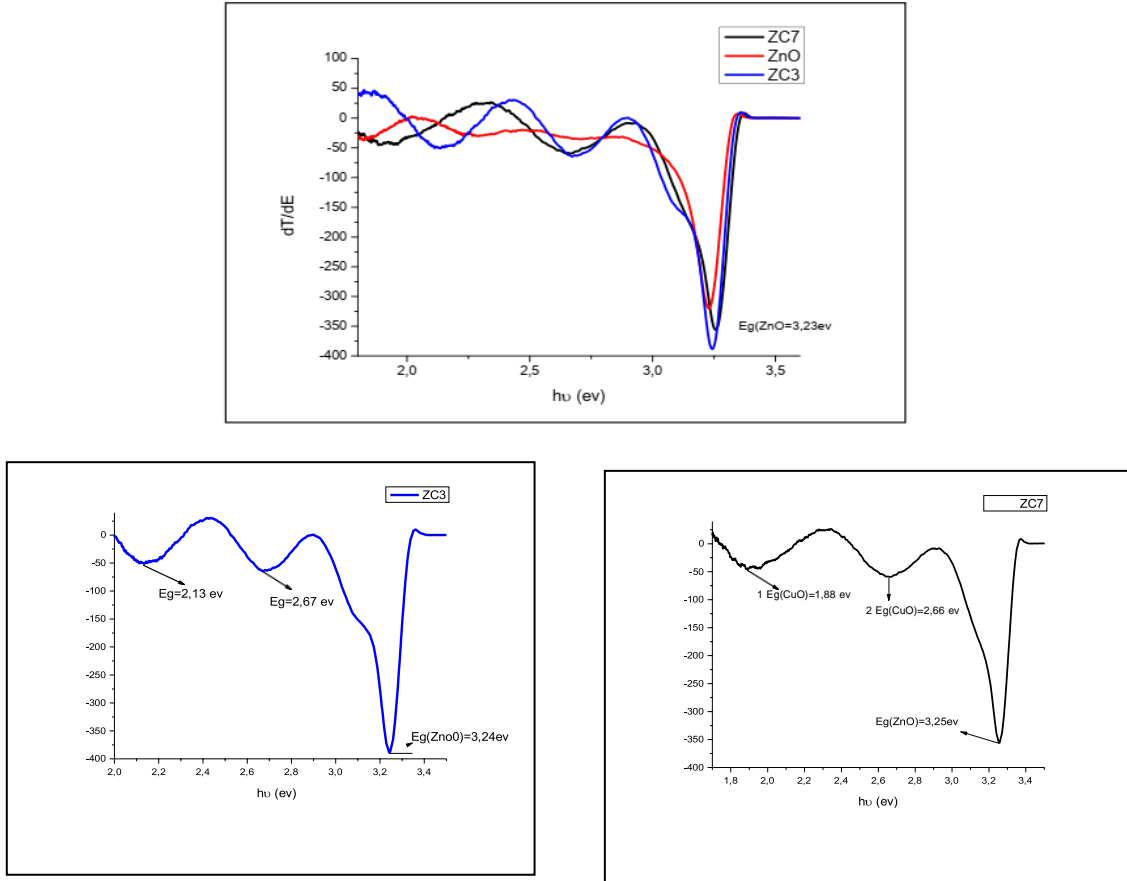
Fig. 3. Plots of the derivative of transmittance (dT/dE) with respect to energy (hv) of ZC0, ZC3, and ZC7 thin films.

The band gap in optics Tauc's approach may be used to derive E_g from the transmittance spectra. To compute the band gap E_g, the well-known Tauc and Beer-Lambert equation was utilized [22]:

$$\alpha h v = A\left(h v - E_g\right)^n \qquad (5)$$

where A is the direct transition constant and h is the photon energy (in eV). The value of can be either of the following: 1/2, 2, 3/2, or 3, depending on whether the shift is indirect.

The optical band gap values of the samples can be obtained by plotting a graph of $(\alpha h)^{1/2}$ versus h and extrapolating $(\alpha h)^{1/2}$ by a straight line = 0. This is seen in Fig.4
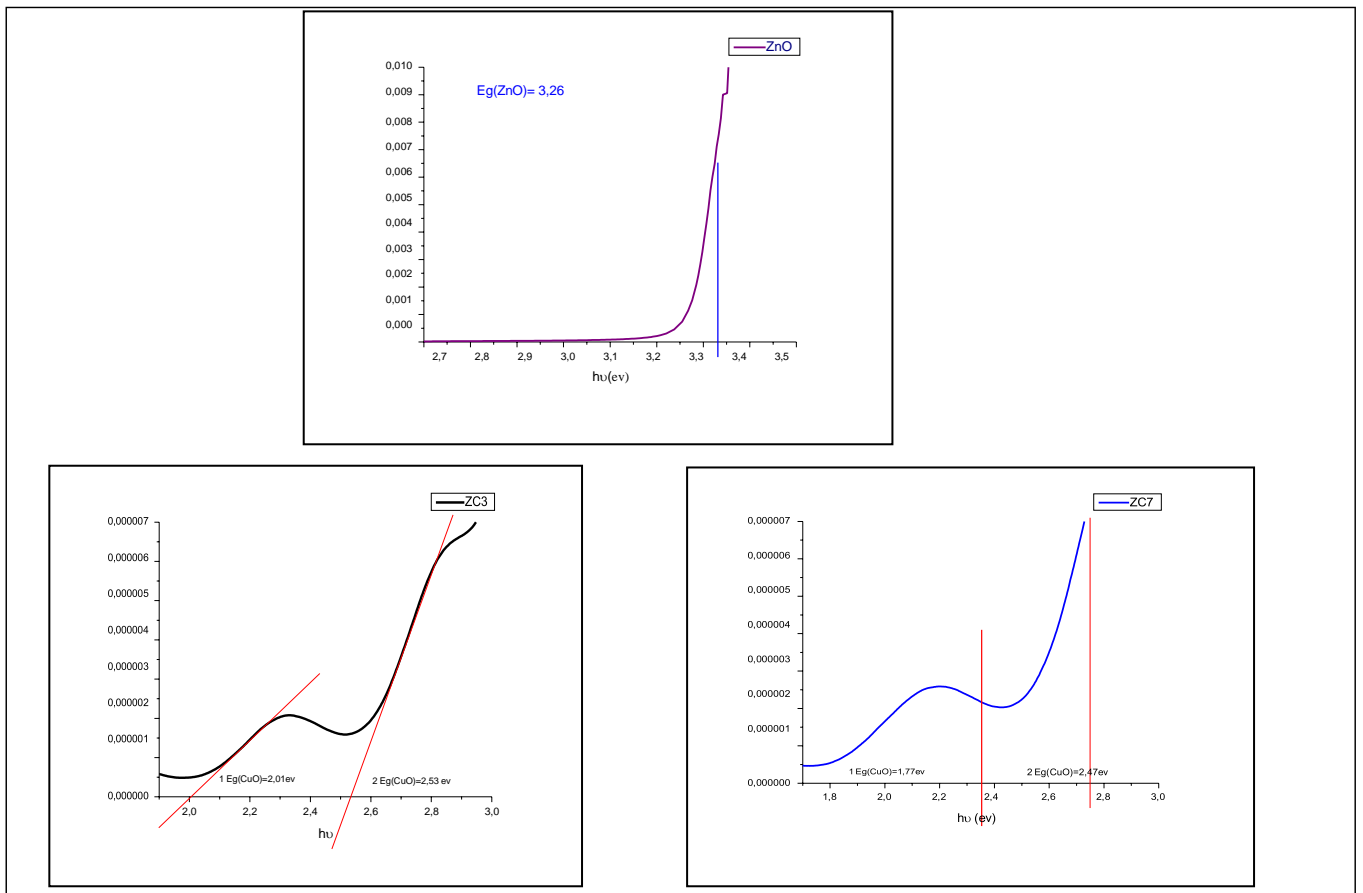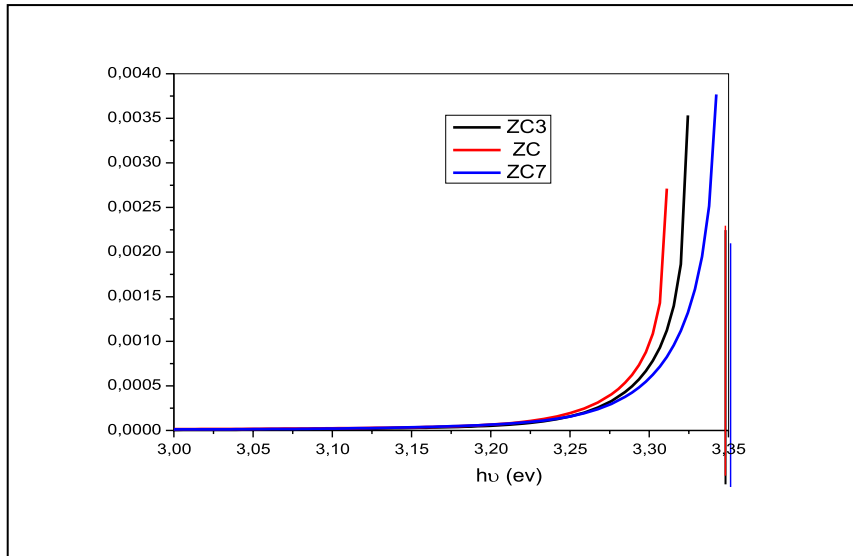
Fig. 4. Plots of (αhv)2 with respect to the energy (hv) of ZC0, ZC3, and ZC7 thin films.

.

	Méthode 1 (dérivé) E_g (eV)	Méthode 2 (Tauc) E_g (eV)
ZC7	ZnO=3.25	ZnO=3.28
	Cu=2.66	Cu=2.47
	Cu=1.88	Cu=1.78
ZC3	ZnO=3.24	ZnO=3.27
	Cu=2.67	Cu=2.53
	Cu=2.13	Cu=2.01
ZC0	3.23	3.26

Table 3. Variations in each sample's optical band gap when placed on glass substrates

Table 3 lists the optical band gap values for each sample.

3.3 Characterization by Spectroscopy of black lines (m-lines)

The observation of the spectra obtained according to the different molar percentages reveals that all the thin layers (ZnO, ZC3 and ZC7) are two modes for the two polarizations TE and TM (Figure 4) This confirms that the layer deposition technique thin Spray pyrolyses makes it possible to manufacture good quality waveguides based on of ZnO.
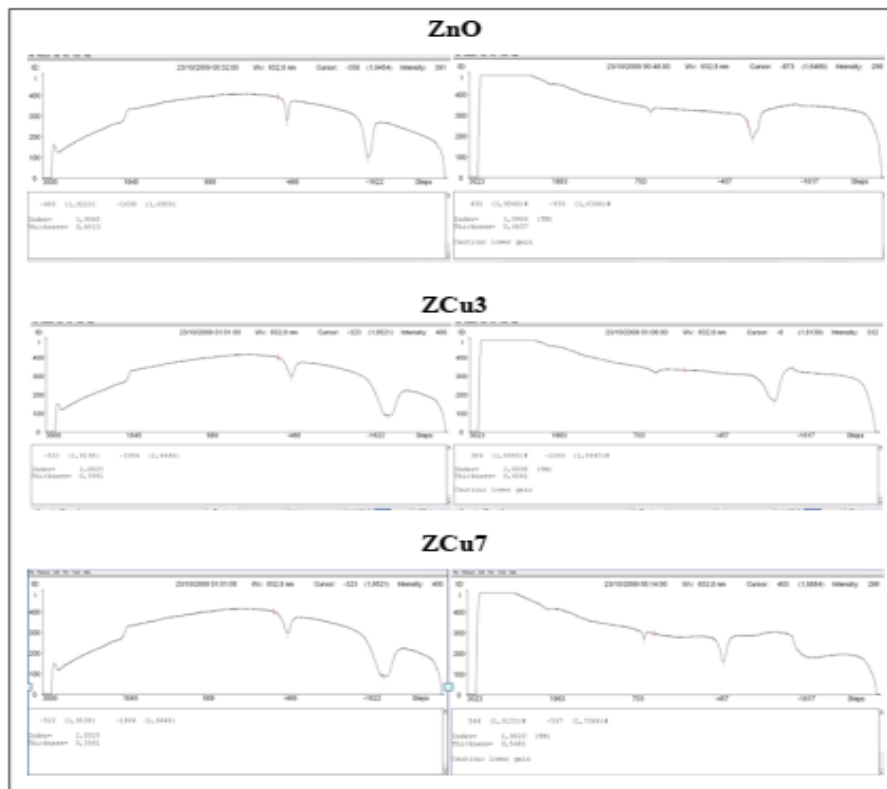
Fig.5. TE and TM guided optical modes in ZnO, ZC3 and ZC7 thin films.

The results of the spectroscopy of the m-lines: The observation of the spectra obtained in function of the different molar percentages reveals that all the thin layers (ZnO, ZC3 and ZC7) are two modes for both TE and TM polarizations.

4.CONCLUSIONS

Studies on the optical and compositional properties of ZnO-ZnO composite nanocomposite films made by spray pyrolysis were carried out. ZnO films exhibit a strong c-axis orientation and a hexagonal wurtzite structure with good crystalline quality, according to XRD research.

The results of the black line spectroscopy: The observation of the spectra obtained according to the different molar percentages reveals that all the thin films (ZnO, ZC3 and ZC7) are two modes for the two polarizations TE and TM. This confirms that the Spray pyrolysis thin film deposition technique allows the manufacture of good quality waveguides based on ZnO. ZC films are characterized by an average optical transmission of [73-83%] in the visible region. With a maximum value of T measured in the ZC7 film.

The values of the forbidden energies vary between (2.2 and 2.4 eV) for CuO and between 3.23 and 3.25 eV) for ZnO. We notice the gap energy of ZnO increases when the concentration of CuO increases.

CONFLICTS OF INTEREST

There are no conflicts of interest, according to the authors.

REFERENCES

[1] G. C. Li, P. F. Liu, R. Liu, M. Liu, K. Tao, S. R. Zhu, M. K. Wu, F. Y. Yi, and L. Han, Dalton Trans. 45,13311 (2016).

[2] J. Yang, D. Zeng, H. Zheng, Q. Xie, J. Huang, L. Xiao, and D.-L. Peng, J. Alloys Compd. 765, 1158 (2019).

[3] Q. Zeng, J. Feng, X. Lin, Y. Zhao, H. Liu, S. Wang, Z. Dong, and W. Feng, J. Alloys Compd. 815, 150550 (2020).

[4] Y. Aoun, R. Meneceur, S. Benramache, and B. Maaoui, Phys. Solid State 62, 131 (2020).

[5] Q. Zhou, W. Zeng, W. Chen, L. Xu, R. Kumar, and A. Umar, Sens. Actuators, B 298, 126870 (2019).

[6] J. Huang, B. Li, Y. Hu, Xi. Zhou, Z. Zhang, Y. Ma, K. Tanga, L. Wang, and Y. Lu, Surf. Coat. Technol.362, 57 (2019).

[7] J. Kim, A. Mirzaei, J. H. Bang, H. W. Kim, and S. S. Kim, Sens. Actuators, B 300, 126981 (2019).

[8] P. Srinivasan, D. Prakalya, and B. G. Jeyaprakash, J. Alloys Compd. 819, 152985 (2020).

[9] Y. Aoun, R. Meneceur, S. Benramache, and B. Maaoui, Phys. Solid State 62, 131 (2020).

[10] E. Barrera-Calva, J.Méndez-Vivar, M. Ortega-López, L. Huerta-Arcos, J. Morales-Corona, R. Olayo-González, Silica-copper oxide composite thin films as solar selective coatings prepared by dipping SolGel, Research Letters in Materials Science (2008) ID 190920 (5pp).

[11] M. Lamri Zeggar, Cupric Oxide thin films deposition for gas sensor application, Thèse de doctorat, Université de Frères Mentouri-Constantine (2016).

[12] Y. Wang, Controllable growth, microstructure and electronic structure of copper oxide thin films, Thèse de doctorat, Université de Lorraine (2015).

[13]. B. Rahal, B. Boudine, Y. Larbah, L. Guerbous, M. Sebais, O. Halimi, and M. Siad, Optik 169, 303 (2018).

[14] A. Taabouche, A. Bouabellou, F. Kermiche, F. Hanini, C. Sedrati, Y. Bouachiba, and C. Benazzouz, Ceram. Int. 42, 6701 (2016).

[15] A. Taabouche, A. Bouabellou, F. Kermiche, F. Hanini, Y. Bouachiba, A. Grid, and T.Kerdja, Mater. Sci. Semicond. Process. 28, 54 (2014).

[16] H. Wang, L. Yuan, and J. An, Crystals. 7, 103 (2017)

[17] B. R. Rehani1, P B Joshi1, K. N. Lad, A. Pratap. INDIAN J PURE & APPL PHYS, 157-161 (2006).

[18] G. Brahim, A. Taabouche, M. Brella, R. Gheriani, Y. Bouachiba, A. Bouabellou, F. Hanini, S. Barouk, H. Serrar, and B. Rahal. Semiconductors, 1063-7826 (2021).

[19] M. Dehimi, T. Touam, A. Chelouche, F. Boudjouan, D. Djouadi, J. Solard, A. Fischer, A. Boudrioua, and A. Doghmane, Adv. Condens. Matter Phys. 2015, 1(2015).

[20] A. Chelouche, T. Touam, M. Tazerout, D. Djouadi, and F. Boudjouan, J. Lumin. 188, 331 (2017).

[21] S. Khodja, T. Touam, A. Chelouche, F. Boudjouan, D. Djouadi, Z. Hadjoub, A. Fischer, and A. Boudrioua, Superlatt. Microstruct. 75, 485 (2014).

[22]M. Brella1, A. Taabouche, B. Gharbi1, R. Gheriani1, Y. Bouachiba4, A. Bouabellou, H. Serrar, S. Touil, K. Laggoune, M. Boudissa. Semiconductors, 1063-7826 (2022)